The Astrophysical Journal, 668: L95–L98, 2007 October 20

TESTING THE EXTERNAL-SHOCK MODEL OF GAMMA-RAY BURSTS USING THE LATE-TIME SIMULTANEOUS OPTICAL AND X-RAY AFTERGLOWS

Yuji Urata,[1] Ryo Yamazaki,[2] Takanori Sakamoto,[3] Kuiyun Huang,[4] Weikang Zheng,[5] Goro Sato,[3] Tsutomu Aoki,[6] Jinsong Deng,[5] Kunihito Ioka,[7] WingHuen Ip,[8] Koji S. Kawabata,[9] YiHsi Lee,[8] Xin Liping,[5] Hiroyuki Mito,[6] Takashi Miyata,[6] Yoshikazu Nakada,[6] Takashi Ohsugi,[2,9] Yulei Qiu,[5] Takao Soyano,[6] Kenichi Tarusawa,[6] Makoto Tashiro,[1] Makoto Uemura,[9] Jianyan Wei,[5] and Takuya Yamashita[8]

Received 2007 July 18; accepted 2007 August 31; published 2007 October 4

ABSTRACT

We study the "normal" decay phase of the X-ray afterglows of gamma-ray bursts (GRBs), which follows the shallow decay phase, using the events simultaneously observed in the *R* band. The classical external-shock model—in which neither the delayed energy injection nor time dependency of shock microphysics is considered—shows that the decay indices of the X-ray and *R*-band light curves, $\alpha_{\rm X}$ and α_o, obey a certain relation, and that in particular, $\alpha_o - \alpha_{\rm X}$ should be larger than $-1/4$ unless the ambient density increases with the distance from the central engine. For our selected 14 samples, we have found that four events violate the limit at more than the 3 σ level, so that a fraction of events are outliers of the classical external-shock model at the "normal" decay phase.

Subject headings: gamma rays: bursts — gamma rays: observations

1. INTRODUCTION

Gamma-ray bursts (GRBs) consist of two phases: prompt GRB emission and subsequent afterglows. How long the prompt GRB emission lasts and when the transition from the prompt GRB to the afterglow occurs have been long-standing problems. These problems are tightly related to the mechanism of the central engine of GRBs. The *Swift* satellite has brought us early, dense, and detailed data on the afterglows of GRBs in various observation bands. Now we are entering the era of multiwavelength observations, especially optical and X-ray bands, which tell us some hints for answering the problems.

Contrary to the expectation in the pre-*Swift* era, *Swift* X-Ray Telescope (XRT) data have revealed complex temporal behavior of the X-ray afterglow (Burrows et al. 2005; Tagliaferri et al. 2005; Nousek et al. 2006; O'Brien et al. 2006a; Willingale et al. 2007). Initially, it decays very steeply, the most popular interpretation of which is the tail emission of the prompt GRB (Kumar & Panaitescu 2000; Zhang et al. 2006; Yamazaki et al. 2006), although other possibilities have been proposed (e.g., Zhang et al. 2007). At several hundreds of seconds after the burst trigger, the shallow decay phase begins and continues until $\sim 10^4$ s, whose origin is quite uncertain (e.g., Toma et al. 2006; Ioka et al. 2006; Zhang 2007). After the shallow decay phase ends, the X-rays subsequently decay, with the decay index usually steeper than unity, which was expected in the pre-*Swift* era. This decay behavior can be well explained by the classical external-shock model (Sari et al. 1998), in which neither the delayed energy injection nor time dependency of shock microphysics is considered. Hence this phase is sometimes called "the normal decay phase."

However, as the number of X-ray observations increases, it is becoming questionable as to whether the normal decay phase arises from the external shock. In the steep and the shallow decay phases, the X-ray light curves sometimes possess large bumps, called "X-ray flares" (Chincarini et al. 2007; Falcone et al. 2007), and/or dips that cannot be explained by the external-shock model (Ioka et al. 2005). Furthermore, for an extreme example, GRB 070110 showed a rather complex X-ray afterglow with a sudden drop at $\sim 2 \times 10^4$ s after the burst trigger as the end of the shallow decay phase (Troja et al. 2007). These observational facts may tell us that the steep and the shallow decay phases are likely due to late internal dissipation of the energy produced by the long-acting central engine. On the other hand, the X-ray spectrum remains unchanged across the shallow-to-normal transition (Nousek et al. 2006), which may imply that the shallow and the normal decay phases are of the same origin. Therefore, it might be that the normal phase comes from the internal energy dissipation.

The observed optical afterglow is also complicated, and in an early epoch ($\lesssim 10^3$ s), there is a diversity (Zhang 2007; Doi et al. 2007). On the other hand, it was found in the pre-*Swift* era that for almost all events, the behavior at $\gtrsim 0.1$ day after the burst could be well explained by the "classical" external-shock model (e.g., Panaitescu & Kumar 2001; Urata et al. 2003), although some events showed complex light curves with dips and/or bumps (e.g., Holland et al. 2003; Lipkin et al. 2004; Urata et al. 2007b). This epoch corresponds to the normal decay phase of the X-ray afterglow. Those previous studies are mainly based on the optical bands, because the X-ray observation was sparse at that time. In the *Swift* era, we are starting to have the simultaneous optical and X-ray afterglow data in the epoch $\gtrsim 0.1$ day after the burst thanks to the rapid and the dense X-ray observation by the XRT.

In this Letter, we study the normal decay phase of the X-

[1] Department of Physics, Saitama University, Shimo-Okubo, Saitama 338-8570, Japan; urata@heal.phy.saitama-u.ac.jp.
[2] Department of Physics, Hiroshima University, Higashi-Hiroshima, Hiroshima 739-8526, Japan; ryo@theo.phys.sci.hiroshima-u.ac.jp.
[3] NASA Goddard Space Flight Center, Greenbelt, MD 20771.
[4] Academia Sinica Institute of Astronomy and Astrophysics, Taipei 106, Taiwan.
[5] National Astronomical Observatories, Chinese Academy of Sciences, Beijing 100012, China.
[6] Kiso Observatory, Institute of Astronomy, University of Tokyo, Kisomuchi, Kiso-gun, Nagano 397-0101, Japan.
[7] Departments of Physics, Kyoto University, Kitashirakawa, Sakyo-ku, Kyoto 606-8602, Japan.
[8] Institute of Astronomy, National Central University, Chung-Li 32054, Taiwan.
[9] Astrophysical Science Center, Hiroshima University, Higashi-Hiroshima, Hiroshima 739-8526, Japan.

ray afterglows simultaneously observed in the optical *R* band, and investigate whether it is consistent with the classical external-shock model or not. We perform a simple test using the optical and the X-ray decay indices, α_o and α_X, where we use a notation $F_\nu \propto t^{-\alpha}\nu^{-\beta}$. For example, in the classical external-shock model with uniform ISM, they are related to the power-law index of the electron distribution, $p(>2)$, as $\alpha_o = 3(p-1)/4$ and $\alpha_X = (3p-2)/4$, respectively, since the cooling frequency ν_c usually lies between the optical and X-ray bands (Sari et al. 1998). Eliminating p, we obtain $\alpha_o - \alpha_X = -1/4$. Similarly, for the wind environment, we derive $\alpha_o - \alpha_X = 1/4$ (Chevarier & Li 2000). These relations between α_o and α_X are also valid in the case of $1 < p < 2$ (Dai & Cheng 2001). Therefore, through the relation between α_o and α_X, one can test the classical external-shock model. In the pre-*Swift* era, similar study has been done for *BeppoSAX* GRBs (De Pasquale et al. 2006). However, compared with the *Swift* GRBs, their X-ray data were not well enough to identify the normal decay phase and to determine the decay index with small uncertainties. We can now obtain more dense X-ray and optical data and can determine α_o and α_X with much less ambiguity. Finally, we note that in this Letter, we do not consider the spectral indices β_o and β_X, because they have at present large uncertainties; β_o fairly depends on the assumed dust model, and the low X-ray flux at the epoch we are interested in makes it difficult to constrain β_X with precision we need to test the model.

2. DECAY INDICES OF THE X-RAY AND *R*-BAND AFTERGLOWS IN THE NORMAL DECAY PHASE

We consider long GRBs that are followed up by *Swift* XRT from the beginning of 2005 to the end of 2006. The *Swift* XRT data are systematically analyzed using our pipeline script. The cleaned event data of the Window Timing (WT) and the Photon Counting (PC) mode from the *Swift* Science Data Center (SDC) are used in the whole process. Although both WT and PC mode data are processed in the pipeline, hereafter we are only focusing on the process of the PC mode data. The search of the X-ray afterglow counterpart, a construction of the X-ray light curve, and a fitting process of the X-ray light curve and spectra are performed automatically using the standard XRT software and calibration database (HEASoft 6.2 and CALDB 20070531). The source region is selected as a circle of 47″ radius. The background region is an annulus of an outer radius of 150″ and an inner radius of 70″, excluding the background X-ray sources detected by `ximage` in circle region of 47″ radius. The light curve is binned based on the number of photons required to meet at least 5 σ (Sakamoto et al. 2007). We select the samples of the X-ray afterglows that have a smooth transition from the shallow to the normal decay phases at $\gtrsim 10^3$ s. Samples with X-ray flares have been excluded. Then we find the start time of the normal decay phase of the X-ray afterglow ($\alpha_X \gtrsim 1$), and extract events in which well-sampled *R*-band light curves are available during the normal decay phase.

The light curve data in the *R* band are published in literatures or observed by the East Asian GRB Follow-up Network (EAFON; Urata et al. 2005)[10] and the Kanata telescope. The *R*-band data taken by us are processed as in the following. A standard routine, including bias subtraction, dark subtraction, and flat-fielding corrections with appropriate calibration data, is employed to process the data using IRAF. Flux calibrations are performed using the APPHOT package in IRAF, referring to the standard stars suggested by Landolt (1992). For each data set, the one-dimensional aperture size is set to 4 times as large as the full width at half-maximum of the objects. The magnitude of error for each optical image is estimated as $\sigma_e^2 = \sigma_{\rm ph}^2 + \sigma_{\rm sys}^2$, where $\sigma_{\rm ph}$ represents the photometric errors for each afterglow, estimated from the output of IRAF PHOT, and $\sigma_{\rm sys}$ is the photometric calibration error estimated by comparing our instrumental magnitudes. When we combine data which are obtained at several different sites, we recalibrate each data set by our photometric manner (e.g., Huang et al. 2007; Urata et al. 2003, 2007a). These efforts decrease systematic differences and yield realistic light curves.

There are 14 GRBs that have good coverage with both X-ray and optical bands at the normal decay phase. Among them, optical data of 11 events have been already published in the literature. For unpublished data obtained by EAFON, detailed light curves in the X-ray and the optical bands are presented elsewhere (Y. Urata et al. 2007, in preparation). For those samples, we identify the normal decay phase that is well described by a single-power-law decay model and derive α_X. During the phase, we find that the optical light curves are well fitted with a single-power-law model in the time interval shown in Table 1 in which the decay index α_o is determined. All results are summarized in Table 1. Figure 1 shows α_o as a function of α_X, while Figure 2 shows the value of $\alpha_o - \alpha_X$ for each event. The quoted errors in this Letter are at the 1 σ confidence level.

3. RESULTS AND DISCUSSION

Let us consider the case of the minimum frequency ν_m smaller than the *R*-band frequency ν_R ($\nu_m < \nu_R$), which is a reasonable assumption for several bright bursts in the pre-*Swift* era. In this case, the spectral index of the optical afterglow is positive, $\beta_o > 0$, which is consistent with the previous observational results (see Table 2 of Kann et al. 2006). The decay and the spectral indices are calculated as shown in Table 2 by the classical external-shock model with ambient matter density dependent on the radius, $n \propto r^{-s}$, where we assume $s > 0$. Since the Lorentz factor of the relativistically expanding shell evolves with the observer time as $\Gamma \propto t^{-(3-s)/(8-2s)}$, $s < 3$ is needed in order for the shell to decelerate. If $\nu_m < \nu_R < \nu_c < \nu_X$, we derive

$$\alpha_o - \alpha_X = -\frac{1}{4} + \frac{s}{8-2s},$$

which is valid for $1 < p < 2$ or $2 < p$, so that $\alpha_o - \alpha_X$ ranges between $-1/4$ and $5/4$ if $0 < s < 3$. For the cases of $\nu_m < \nu_R < \nu_X < \nu_c$ or $\nu_m < \nu_c < \nu_R < \nu_X$, $\alpha_o - \alpha_X$ should be zero. As can be seen in Figure 2, among 14 events considered in this Letter, four events (GRB 050319, 050401, 060206, 060323) are below the line $\alpha_o - \alpha_X = -1/4$ at more than the 3 σ level, so that a fraction of bursts are outliers of the classical external-shock model at the normal decay phase. De Pasquale et al. (2006) have performed similar study and found two out of 12 events have $\alpha_o - \alpha_X$ significantly below $-1/4$, which was roughly consistent with our result (see Table 5 of their paper).

Liang et al. (2007) studied the α_X-β_X relation of the normal decay phase and found that there are several outliers of the classical external-shock model. Their outliers have large $\alpha_X > 2$. In our sample, however, outliers of α_o-α_X relation exists even if their α_X is around 1.5, and their α_X-β_X relations are

[10] In this Letter, the samples are mainly taken using the Kiso 1.05 m Schmidt telescope (Urata et al. 2003), Lulin 1 m telescope (Huang et al. 2005), and Xinglong 0.8 m telescope (Deng et al. 2007).

TABLE 1

X-RAY AND OPTICAL TEMPORAL DECAY INDICES DURING X-RAY NORMAL DECAY PHASE.

GRB	Normal Decay Phase[a] (s)	Optical Period[b] (s)	α_X	α_o	$\alpha_o - \alpha_X$	References
050319_1	4.8×10^4–2.0×10^6	1.3×10^5–4.1×10^5	1.52 ± 0.13	0.48 ± 0.02	-1.04 ± 0.13	1
050319_2	4.8×10^4–2.0×10^6	4.1×10^5–9.9×10^5	1.52 ± 0.13	2.45 ± 0.18	0.93 ± 0.22	1
050401	3.4×10^3–6.3×10^5	3.5×10^3–1.4×10^5	1.39 ± 0.06	0.76 ± 0.03	-0.63 ± 0.07	2
050408_1	2.6×10^3–3.2×10^6	3.4×10^3–4.6×10^4	0.86 ± 0.01	0.59 ± 0.03	-0.27 ± 0.03	1, 3
050408_2	2.6×10^3–3.2×10^6	6.2×10^4–3.0×10^5	0.86 ± 0.01	0.98 ± 0.09	0.12 ± 0.09	1, 3
050525A_1	3.1×10^3–2.7×10^6	3.1×10^3–5.7×10^4	1.51 ± 0.04	1.25 ± 0.04	-0.26 ± 0.06	1, 4, 5
050525A_2	3.1×10^3–2.7×10^6	6.3×10^4–4.6×10^5	1.51 ± 0.04	1.53 ± 0.09	0.02 ± 0.10	1, 4, 5
050721_1	2.3×10^3–3.4×10^6	2.3×10^3–7.9×10^3	0.96 ± 0.09	1.23 ± 0.03	0.27 ± 0.09	6
050721_2	2.3×10^3–3.4×10^6	7.9×10^3–2.5×10^5	0.96 ± 0.09	0.54 ± 0.06	-0.42 ± 0.11	6
050801	6.5×10^2–3.0×10^5	7.2×10^2–9.5×10^3	0.99 ± 0.04	1.04 ± 0.03	0.05 ± 0.05	7
050820A	2.8×10^3–4.0×10^4	3.4×10^3–2.0×10^4	1.04 ± 0.02	0.73 ± 0.04	-0.31 ± 0.04	8
050824	5.9×10^4–2.0×10^6	8.0×10^4–4.5×10^5	0.85 ± 0.06	0.51 ± 0.03	-0.34 ± 0.07	9
051109A_1	1.6×10^3–5.2×10^4	1.6×10^3–1.3×10^4	1.08 ± 0.02	0.66 ± 0.06	-0.42 ± 0.06	10
051109A_2	5.2×10^4–1.4×10^6	9.0×10^4–1.0×10^6	1.35 ± 0.03	0.98 ± 0.06	-0.37 ± 0.07	10
060206_1	2.3×10^4–5.4×10^5	2.3×10^4–2.5×10^4	1.39 ± 0.08	0.86 ± 0.03	-0.53 ± 0.09	1, 11, 12
060206_2	2.3×10^4–5.4×10^5	2.5×10^4–2.0×10^5	1.39 ± 0.08	1.41 ± 0.02	0.02 ± 0.08	1, 11, 12
060323	1.1×10^3–2.1×10^5	1.2×10^3–3.0×10^3	1.38 ± 0.10	0.70 ± 0.05	-0.68 ± 0.11	1
060526	1.8×10^4–4.2×10^5	2.0×10^4–3.2×10^4	1.60 ± 0.13	1.17 ± 0.07	-0.43 ± 0.15	13
060605	5.2×10^3–2.7×10^4	2.0×10^4–2.3×10^4	1.45 ± 0.06	1.41 ± 0.44	-0.04 ± 0.44	1
061121_1	2.1×10^3–1.7×10^4	4.7×10^3–1.5×10^4	0.98 ± 0.04	0.98 ± 0.05	0.00 ± 0.06	14
061121_2	1.7×10^4–3.5×10^5	7.2×10^4–3.3×10^5	1.46 ± 0.03	1.54 ± 0.07	0.08 ± 0.08	14, 15

[a] The normal decay phase is identified in the *Swift* XRT data. The value of α_X is determined in this period. Time zero is taken as the burst trigger time.

[b] The period when the optical data was taken during the normal decay phase. The value of α_o is determined in this epoch.

REFERENCES FOR OPTICAL DATA.—(1) EAFON (for specific individual events, e.g., Huang et al. 2007; Deng et al. 2007); (2) De Pasquale et al. 2006; (3) de Ugarte Postigo et al. 2007; (4) Klotz et al. 2005; (5) Della Valle et al. 2006; (6) Antonelli et al. 2006; (7) Rykoff et al. 2006; (8) Cenko et al. 2006; (9) Sollerman et al. 2007; (10) Yost et al. 2007; (11) Woźniak et al. 2006; (12) Stanek et al. 2007; (13) Dai et al. 2007; (14) Uemura et al. 2007; (15) Halpern et al. 2006.

consistent with the classical external-shock model (see Fig. 5 of Liang et al. 2007). This fact, therefore, strengthens the importance of the multiwavelength studies at the normal decay phase to test the classical external-shock model.

There are several possibilities leading to $\alpha_o - \alpha_X < -1/4$. One is to consider the $s < 0$ case (e.g., Yost et al. 2003). If $s \lesssim -4$, then $\alpha_o - \alpha_X \lesssim -0.5$; however, there is no theoretical reason to consider such a steeply rising profile. Another possibility is to consider the delayed energy injection (Rees & Mészáros 1998) and/or time-variable shock microphysics parameters (Yost et al. 2003). Here we consider $\nu_m < \nu_R < \nu_c < \nu_X$ for simplicity. The generalized forms of α_o and α_X are then derived by Panaitescu et al. (2006) based on the assumptions $E(>\Gamma) \propto \Gamma^{-e}$, $\epsilon_B \propto \Gamma^{-b}$, $\epsilon_e \propto \Gamma^{-i}$, and $n \propto r^{-s}$, where $s < 3$. Then, from their derived formula, we obtain

$$\alpha_o - \alpha_X = -\frac{1}{4} + \frac{s}{8-2s} - \frac{3-s}{4(e+8-2s)}\left(\frac{4-3s}{4-s}e + 3b\right), \quad (1)$$

which is independent of i and p. We find that $\alpha_o - \alpha_X < -1/4$ is achieved if $e + 3b > 0$ for the uniform ISM case ($s = 0$), or

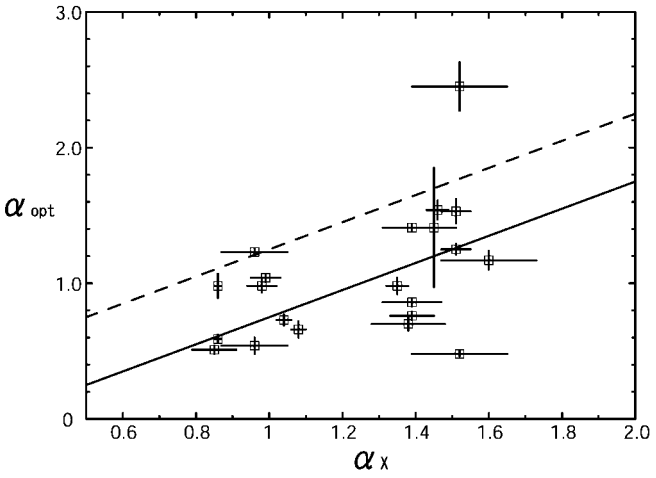

FIG. 1.—*R*-band decay index α_o as a function of the X-ray decay index α_X in the normal decay phase. The classical external-shock model predicts $\alpha_o - \alpha_X = -1/4$ (*solid line*) and 1/4 (*dashed line*) for the uniform ISM ($s = 0$) and for the wind medium ($s = 2$) cases, respectively.

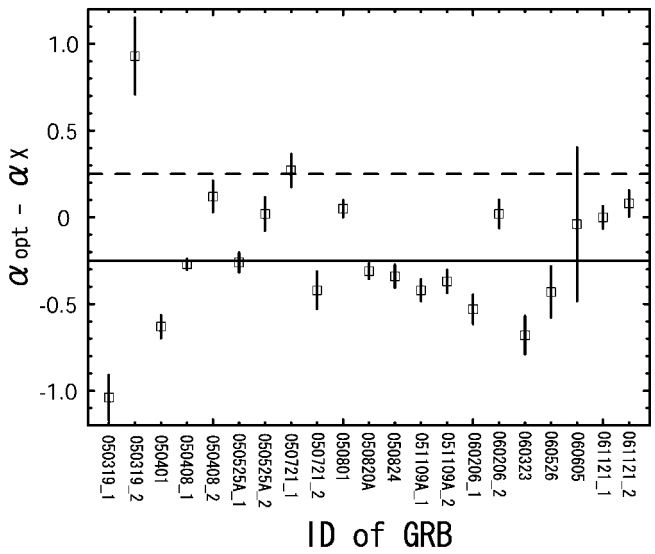

FIG. 2.—Range of $\alpha_o - \alpha_X$ for individual events. The meanings of the solid and the dashed lines are the same as those in Fig. 1.

TABLE 2
SPECTRAL AND DECAY INDICES ($F_\nu \propto t^{-\alpha}\nu^{-\beta}$) PREDICTED BY THE CLASSICAL EXTERNAL-SHOCK MODEL

	$1 < p < 2$		$2 < p$	
ν	α	β	α	β
$\nu < \nu_m$	$[(4s - 3)p - 2(s + 3)]/[3(p - 1)(8 - 2s)]$	$-1/3$	$(s - 2)/(4 - s)$	$-1/3$
$\nu_m < \nu < \nu_c$	$[(3 - s)p + (6 + s)]/[2(8 - 2s)]$	$(p - 1)/2$	$(3p - 1)/4 + s/(8 - 2s)$	$(p - 1)/2$
$\nu_c < \nu$	$[(3 - s)p + 2(5 - s)]/[2(8 - 2s)]$	$p/2$	$(3p - 2)/4$	$p/2$

NOTES.—This is for the case of spherical expansion, slow cooling, and the ambient density profile given by $n \propto r^{-s}$, where $0 < s < 3$. The break frequency ν_m evolves with time as $\nu_m \propto t^{-3/2}$ for $2 < p$, while $\nu_m \propto t^{-[(3-s)p+6-s]/[(p-1)(8-2s)]}$ for $1 < p < 2$, and ν_c scales as $\nu_c \propto t^{(3s-4)/(8-2s)}$ regardless of p.

if $b - e > 8/3$ for the wind medium case ($s = 2$). Note that these cases have been discussed for the pre-*Swift* GRBs (Piro et al. 1998; Yost et al. 2003; Corsi et al. 2005).

Another possibility to explain the outliers may be that the X-ray flares superposing on the X-ray afterglow could steep the apparent decay index of the X-ray. X-ray flares are usually more active in the initial phase, so that they may enhance the early X-ray flux. In this case the X-ray flare should not be spiky but relatively smooth, and the late afterglow is just an ordinary afterglow.

Although the external-shock model is still viable, the afterglow emissions of outliers may be capable of the internal shock origin. Such a possibility has been proposed by Ghisellini et al. (2007). In this case, the optical and X-ray emission in the late phase are of different origins. It is also possible in this model that a chromatic break occurs at ~1 day after the burst, which was believed to be achromatic in the pre-*Swift* era and to be caused by the jet collimation effects (Panaitescu et al. 2006; Huang et al. 2007; Sato et al. 2007). Or a cannonball model may account for our outliers (Dado et al. 2007).

We would like to thank Shiho Kobayashi and Bing Zhang, and the anonymous referee for useful comments. This work was supported in part by Grants-in-Aid for Scientific Research of the Japanese Ministry of Education, Culture, Sports, Science, and Technology 18001842 (Y. U.) and 18740153 (R. Y.). This work was also supported by NSC 93-2752-M-008-001-PAE and NSC 93-2112-M-008-006. T. S. was supported by an appointment of the NASA Postdoctoral Program at the Goddard Space Flight Center, administered by Oak Ridge Associated Universities through a contract with NASA. This Letter was inspired through the discussion during the workshop "Implications of *Swift*'s Discoveries about Gamma-Ray Bursts" at the Aspen Center for Physics.

REFERENCES

Antonelli, L. A., et al. 2006, A&A, 456, 509
Burrows, D. N., et al. 2005, Science, 309, 1833
Cenko, S. B., et al. 2006, ApJ, 652, 490
Chevarier, R. A., & Li, Z.-Y. 2000, ApJ, 536, 195
Chincarini, G., et al. 2007, ApJ, submitted (astro-ph/0702371)
Corsi, A., et al. 2005, A&A, 438, 829
Dado, S., Dar, A., & De Rujula, A. 2007, preprint (arXiv:0706.0880)
Dai, X., et al. 2007, ApJ, 658, 509
Dai, Z. G., & Cheng, K. S. 2001, ApJ, 558, L109
Della Valle, M., et al. 2006, ApJ, 642, L103
Deng, J., et al. 2007, Nuovo Cimento B, in press
De Pasquale, M., et al. 2006, A&A, 455, 813
de Ugarte Postigo, A., et al. 2007, A&A, 462, L57
Doi, H., Takami, K., & Yamazaki, R. 2007, ApJ, 659, L95
Falcone, A. D., et al. 2007, ApJ, in press (arXiv:0706.1564)
Ghisellini, G., et al. 2007, ApJ, 658, L75
Halpern, J. P., et al. 2006, GCN Circ. 5847, http://gcn.gsfc.nasa.gov/gcn/gcn3/5847.gcn3
Holland, S. T., et al. 2003, AJ, 125, 2291
Huang, K. Y., et al. 2005, ApJ, 628, L93
———. 2007, ApJ, 654, L25
Ioka, K., Kobayashi, S., & Zhang, B. 2005, ApJ, 631, 429
Ioka, K., et al. 2006, A&A, 458, 7
Kann, D. A., Klose, S., & Zeh, A. 2006, ApJ, 641, 993
Klotz, A., et al. 2005, A&A, 439, L35
Kumar, P., & Panaitescu, A. 2000, ApJ, 541, L51
Landolt, A. U. 1992, AJ, 104, 340
Liang, E. W., Zhang, B. B., & Zhang, B. 2007, ApJ, in press (arXiv:0705.1373)
Lipkin, Y. M., et al. 2004, ApJ, 606, 381
Nousek, J. A., et al. 2006, ApJ, 642, 389
O'Brien, P. T., et al. 2006a, ApJ, 647, 1213
Panaitescu, A., & Kumar, P. 2001, ApJ, 560, L49
Panaitescu, A., et al. 2006, MNRAS, 369, 2059
Piro, L., et al. 1998, A&A, 331, L41
Rees, M., & Mészáros, P. 1998, ApJ, 496, L1
Rykoff, E. S., et al. 2006, ApJ, 638, L5
Sakamoto, T., et al. 2007, ApJ, submitted
Sari, R., Piran, T., & Narayan, R. 1998, ApJ, 497, L17
Sato, G., et al. 2007, ApJ, 657, 359
Sollerman, J., et al. 2007, A&A, 466, 839
Stanek, K. Z., et al. 2007, ApJ, 654, L21
Tagliaferri, G., et al. 2005, Nature, 436, 985
Toma, K., et al. 2006, ApJ, 640, L139
Troja, E., et al. 2007, ApJ, 665, 599
Uemura, M., et al. 2007, PASJ, submitted
Urata, Y., et al. 2003, ApJ, 595, L21
———. 2005, Nuovo Cimento C, 28, 775
———. 2007a, ApJ, 655, L81
———. 2007b, ApJ, submitted
Willingale, R., et al. 2007, ApJ, 662, 1093
Woźniak, P. R., et al. 2006, ApJ, 642, L99
Yamazaki, R., Toma, K., Ioka, K., & Nakamura, T. 2006, MNRAS, 369, 311
Yost, S. A., et al. 2003, ApJ, 597, 459
———. 2007, ApJ, 657, 925
Zhang, B. 2007, Chinese J. Astron. Astrophys., 7, 1
Zhang, B., et al. 2006, ApJ, 642, 354
Zhang, B. B., Liang, E. W., & Zhang, B. 2007, ApJ, 666, 1002